

# Interstrip Capacitance of the Double-Sided Silicon Strip Detector

K. Yamamoto, M. Muramatsu, K. Yamamura, M. Ohmura, H. Utsuyama, H. Anzai, K. Saito, M. Konmura, M. Nakamura, and K. Niwa

**Abstract**—The signal-to-noise ratio of the silicon strip detector is strongly influenced by the capacitance associated with the readout electronics. From a theoretical study, it is known that the strip geometry of such detectors dominates the strip capacitance. In order to know numerical values of the strip capacitance to estimate the detector performance and to find the best detector structure, we designed and fabricated several dedicated samples. These have different strip geometries and readout methods. The capacitance of each sample device was measured before and after exposure to  $\gamma$ -rays to test the radiation hardness.

## I. INTRODUCTION

SILICON strip detectors have become essential devices for high energy physics experiments [1]–[3]. They have an excellent position resolution, high rate capability and two-track separation capability, which makes them very useful for vertex determination. It is well known that the strip pitch and the type of readout electronics determines the position resolution [4], but the electrical behavior such as the strip capacitance and radiation effects mainly depend on the detector geometry [5], [6]. For the detection of the signal, each strip has to be connected to charge-amplifier frontend electronics specifically designed for these applications. The signal-to-noise ratio of this system is strongly influenced by the capacitance of each strip. Recently, it has become possible to estimate the strip capacitance by theoretical calculations, and experimental results are in good agreement [7]–[9].

To study the design philosophy of the silicon strip detector, we previously tried to find the evaluation methods of the strip capacitance and design parameters for the double-sided strip detectors [10]. By measurements on the fabricated test structure, we had fairly useful information for actual detector designing. This previous work was done with one fixed pitch device. To understand the controlling parameters for the interstrip capacitance, we tried to test a wider variety of strip geometries. For the first experiment, the strip widths were varied three dif-

ferent pitches on the junction side. Some of them had floating strips between the readout strips.

How to keep the good signal-to-noise ratio during the operation is also important. We therefore tested the radiation effects of high energy beam on the strip capacitance.

## II. EXPERIMENT

### A. Detector Design

For the silicon strip detector connected to a charge sensitive amplifier, one has to consider several important parameters to get higher signal-to-noise ratio. The most important thing is to minimize the strip capacitance [11]. It is known that the main components of the strip capacitance are the interstrip capacitance and the backplane capacitance. In the case of the ac coupling strip detector, the coupling capacitor has to be sufficiently larger than the interstrip capacitance to avoid the signal spreading over the strips. This coupling capacitor is dominated by the thickness and area of the insulator between the strip and ac electrode.

Considering this information, we designed several different geometries to find the controlling parameters and absolute values.

- Chip size:  $20 \times 20 \text{ mm}^2$
- Effective area:  $15 \times 16.7 \text{ mm}^2$   
(This includes 18 different patterns)
- Strip pitch:  $24 \mu\text{m}$ ,  $50 \mu\text{m}$ ,  $100 \mu\text{m}$
- Coupling capacitance:  $\approx 2000 \text{ angstrom SiO}_2$
- Design of strip pattern: see Table II.

The strip length is 15 mm and the total width of each pattern is 1 mm. So the number of strips for  $24 \mu\text{m}$  pitch,  $50 \mu\text{m}$  pitch and  $100 \mu\text{m}$  pitch are 40 pieces, 20 pieces, and 10 pieces, respectively.

Each strip has both ac and dc electrodes. We designed three types of detectors with and without floating strips between the readout strips.

Fig. 1 shows the cross sectional schematic views, and each dimension of the photomask pattern is listed in Table I.

### B. Detector Samples

The detectors were fabricated using 3-6 k $\Omega$ -cm high resistive *n*-type wafers. The size of the wafer was 4 in and the thickness was  $300 \pm 10 \mu\text{m}$ . Fig. 2 shows the representative pictures of these devices. All devices were

Manuscript received October 31, 1992; revised June 10, 1993.

K. Yamamoto, M. Muramatsu, K. Yamamura, M. Ohmura, H. Utsuyama, and H. Anzai, are with Hamamatsu Photonics K.K., 1126-1 Ichimocho, Hamamatsu City 435, Japan.

K. Saito, M. Konmura, M. Nakamura, and K. Niwa are with the Department of Physics, Nagoya University, Chikusa-ku, Nagoya, Japan.

This paper was originally presented at the 1991 Nuclear Science Symposium, held in Santa Fe, NM on November 2–9, 1991.

IEEE Log Number 9212324.

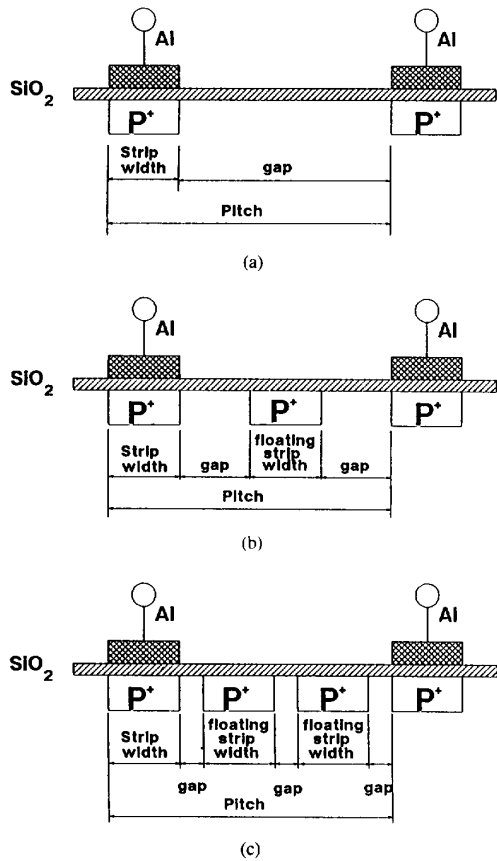


Fig. 1. Cross sectional schematic view (a) Type I. (b) Type II.

TABLE I  
GEOMETRY OF TEST DEVICES

Type no.	Device no.	Pitch	Strip width	Floating width	Gap
I	01	24 $\mu\text{m}$	6 $\mu\text{m}$		18 $\mu\text{m}$
I	02	24	8		16
I	03	24	10		14
I	04	24	14		10
I	05	50	8		42
I	06	50	10		40
I	07	50	16		34
I	08	50	32		18
I	09	100	10		90
I	10	100	20		80
I	11	100	40		60
I	12	100	80		20
II	13	50	8	6 $\mu\text{m}$	18 $\times$ 2
II	14	50	10	10	15 $\times$ 2
III	15	50	10	8 $\times$ 2	8 $\times$ 3
II	16	100	10	10	40 $\times$ 2
II	17	100	10	50	20 $\times$ 2
III	18	100	10	10 $\times$ 2	23 $\times$ 3

mounted on the specially designed G-10 substrates. Electrical connection was done by Aluminum wire bonding.

### C. Exposure

The radiation exposure was performed at the Institute of Nagoya University using  $^{60}\text{CO}$   $\gamma$ -rays. The detectors

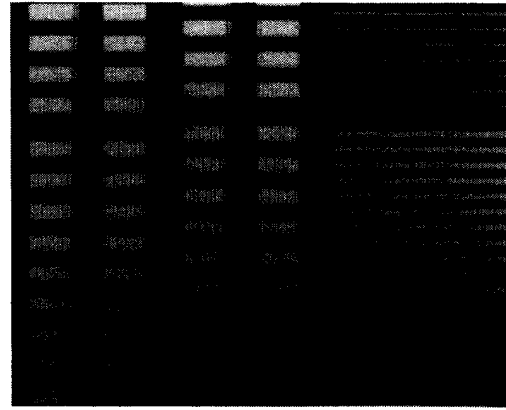


Fig. 2. A microphotograph of detector sample.

were exposed to 1 MeV  $\gamma$ -rays with total dose up to 500 kRad. The ionization current of the strip detector was used as the monitor for the radiation exposure. 80 V bias was supplied to the detector during the irradiation, and the ac electrode was kept as the ground potential.

### D. Capacitance Measurement

Fig. 3 shows the simplified circuit network for the ac coupling strip detector.  $C_b$  is the backplane capacitance,  $C_c$  is the coupling capacitance and  $C_e$  is the ac electrode capacitance. The value of  $C_b$  and  $C_c$  are measured by the conventional methods. The ac interstrip capacitance is the capacitance between the electrode  $E_{A1}$  and  $E_{A2}$ , and the dc interstrip capacitance is the capacitance between  $E_{D1}$  and  $E_{D2}$ .

Fig. 4 shows the ac interstrip capacitance measurement schematically. The capacitance was measured by a charge injection method. One ac electrode is connected to a step voltage source. A neighboring ac electrode is connected to a charge sensitive amplifier. We used a 5 msec step pulse with 10 Hz duty cycle. The readout amplifier time constant was 200  $\mu\text{sec}$ . Plus bias voltage was supplied from  $n$ -substrate. Each set of strips was connected to ground potential through a 5.1 M $\Omega$  bias resistor.

Using the value of the input step voltage ( $V_{in}$ ), charge-amplifier feedback capacitance ( $C_f$ ) and the output voltage ( $V_{out}$ ), the ac interstrip capacitance between the two ac electrodes is calculated:

$$C_{ac} = C_f \times \frac{V_{out}}{V_{in}}$$

We calculated this capacitance as one side interstrip capacitance. So the total strip capacitance should be ( $2C_{ac} + C_b$ ).

The dc interstrip capacitance was measured and calculated almost same method.

## III. RESULTS AND DISCUSSION

Table II shows the results of measuring each capacitance. The coupling capacitance ( $C_c$ ) strongly depends on

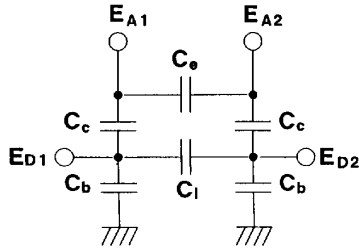


Fig. 3. Simplified circuit network.

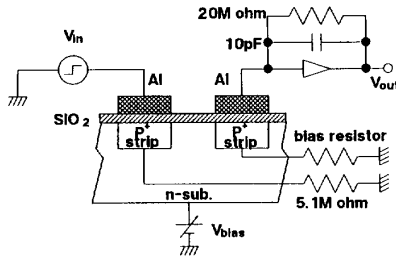


Fig. 4. ac interstrip capacitance measurement.

TABLE II  
MEASURED CAPACITANCE VALUE

Type no.	Device no.	$C_c$ (pF/cm)	$C_b$ (pF/cm)	$C_{dc}$ (pF/cm)	$C_{ac}$ (pF/cm)
I	01	4.7	$\approx 0.1$	0.44	0.27
I	02	7.3	0.1	0.53	0.37
I	03	9.8	0.1	0.59	0.44
I	04	15.0	0.1	0.80	0.63
I	05	8.1	0.18	0.57	0.45
I	06	10.6	0.18	0.63	0.51
I	07	18.4	0.18	0.66	0.61
I	08	38.2	0.18	0.69	0.89
I	09	10.7	0.29	0.47	0.37
I	10	25.0	0.29	0.55	0.53
I	11	52.4	0.29	0.74	0.73
I	12	107.0	0.29	1.08	1.06
II	13	7.9	0.16	0.57	0.43
II	14	10.5	0.16	0.58	0.47
III	15	10.3	0.16	0.56	0.48
II	16	11.2	0.26	0.43	0.37
II	17	11.2	0.26	0.48	0.50
III	18	11.2	0.26	0.47	0.47

the frequency of measurement. In Table II, we selected the capacitance value at 100 kHz, low frequency flat region. This capacitance should be proportional to the width of aluminum ac electrodes. Compared with mask design, the width of aluminum becomes nearly  $2 \mu\text{m}$  narrower because of the side etching. In the case of narrow strip pattern, we have to take care to keep significantly larger  $C_c$  than the total-strip capacitance ( $2C_{ac} + C_b$ ).

Fig. 5 shows the backplane capacitance of 100  $\mu\text{m}$  pitch and 50  $\mu\text{m}$  pitch detector ( $C_b$ ).

$C_b$  depends on the strip pitch, almost the same even if the strip width is different. Higher than the full depletion voltage, this capacitance becomes steady. We measured the value at 100 V bias. Fig. 6 shows  $C_b$  with or without

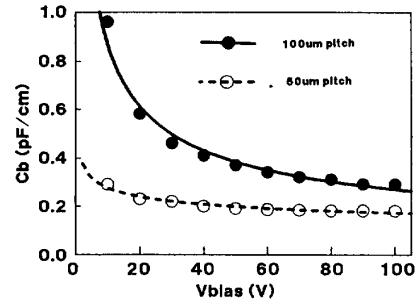


Fig. 5. Backplane capacitance.

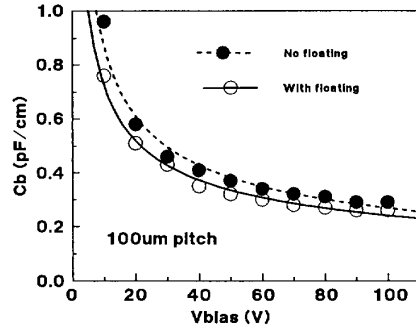


Fig. 6. Backplane capacitance.

floating strips between the readout electrodes. There is only a small difference between these values at full depletion condition.

Fig. 7 shows the ac interstrip capacitance ( $C_{ac}$ ) of 24  $\mu\text{m}$  pitch detector. This capacitance differs with strip geometry (pitch, width, with or without floating strip), but depends less on the bias voltage. Fig. 8 shows the geometry dependency of  $C_{ac}$ . Smaller width and pitch strips have smaller interstrip capacitances. If the width of the strip is the same, the wider gap (wider pitch) detector has the smaller  $C_{ac}$ .

There is almost no difference in the value of  $C_{ac}$  with floating strips or without them. There is a very similar tendency in the dc interstrip capacitance ( $C_{dc}$ ), only the absolute value of  $C_{ac}$  is smaller than  $C_{dc}$ .

Table III summarizes the effects of the radiation exposure on  $C_{ac}$ . After the exposure,  $C_{ac}$  increases by 10–20% depending on the pattern geometry. Other capacitances ( $C_c, C_b$ ) have smaller change than  $C_{ac}$ , but  $C_{dc}$  changes the same amount as  $C_{ac}$ . Fig. 9 shows the comparison of 24  $\mu\text{m}$  pitch detector  $C_{ac}$  before and after the irradiation. Both of the  $C_{ac}$  values are good hits on the straight line. Maybe there is a simple explanation for this  $C_{ac}$  increase after the exposure.

#### IV. CONCLUSION

Capacitance properties of silicon strip detectors were examined with specially designed strip patterns. This time, we measured only the junction side capacitance. Each capacitance of this side has a simple dependency on the

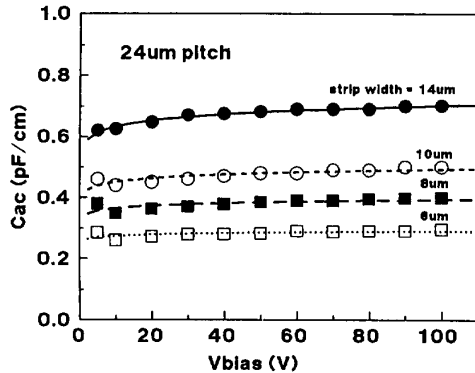
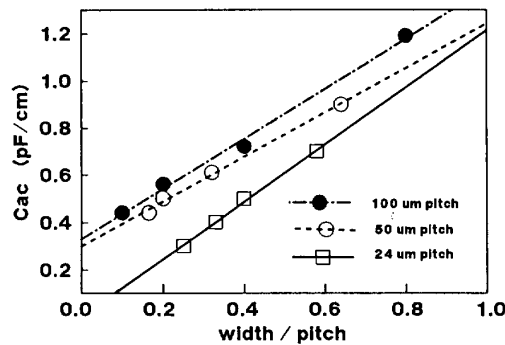


Fig. 7. Interstrip capacitance dependency on the strip width.

Fig. 8. Geometry dependency of  $C_{ac}$ .TABLE III  
EFFECT OF EXPOSURE ON  $C_{ac}$ 

Type no.	Device no.	Before $C_{ac}$ (pF/cm)	After $C_{ac}$ (pF/cm)
I	01	0.30	0.33
I	02	0.50	0.50
I	03	0.60	0.60
I	04	0.89	0.89
I	05	0.52	0.52
I	06	0.58	0.58
I	07	0.77	0.77
I	08	1.18	1.18
I	09	0.44	0.44
I	10	0.65	0.65
I	11	0.89	0.89
I	12	1.40	1.40
II	13	0.44	0.44
II	14	0.49	0.56
III	15	0.50	0.56
II	16	0.46	0.50
II	17	0.46	0.55
III	18	0.45	0.54

strip pattern geometry. It is clear that the interstrip capacitance is dominant to the total capacitance than the backplane capacitance. With these experiments, we found the conclusion that the reduction of the strip width seems to be suitable for reducing the interstrip capacitance. In case of the given desired pitch, this means the largest gap width is preferable.

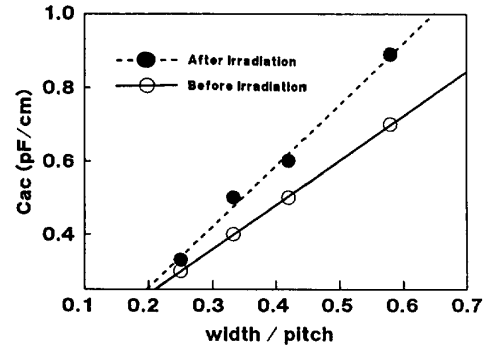


Fig. 9. Radiation effect on the interstrip capacitance.

The effect of the radiation exposure is not significantly high on the capacitance. This means the signal-to-noise ratio should not deteriorate much during the operation.

The interface of Si-SiO<sub>2</sub> accumulates electrons not only naturally but also by the positive ion traps in SiO<sub>2</sub> during the high energy beam exposure. This should be the main reason of the increase of the interstrip capacitance after the radiation exposure.

The floating strip between the readout strips is a useful method to get higher resolution with smaller readout terminals. This is the so-called charge division method. The capacitance value and radiation hardness of these detectors have no difference compared with types with no floating strips.

This paper shows only the junction side test results. We had already designed and fabricated wide variety devices for the test of ohmic side strip characteristics. We want to measure and present the results in the near future.

#### V. ACKNOWLEDGMENT

We wish to thank F-laboratory members of Nagoya University for their technical help, and to Si process group at Hamamatsu Photonics K. K. for the fabrication of the test devices. We also would like to thank Dr. T. Ohsugi, Hiroshima University and Dr. Y. Unno, K. E. K. for their useful discussion and encouragement.

#### REFERENCES

- [1] C. Adolphsen, A. S. Schwarz, M. Turala, and A. Steiner, "A silicon strip vertex detector for the mark II experiment at the SLAC Linear Collider," *Nucl. Instr. Meth.*, vol. A260, p. 124, 1987.
- [2] M. Burns, H. Dijkstra, R. Horisberger *et al.*, "Progress in the construction of the Delphi microvertex detector," *Nucl. Instr. Meth.*, vol. A277, p. 154, 1989.
- [3] C. Haber, W. Carithers, R. P. Ely *et al.*, "Design and prototyping of the front end readout system for the CDF silicon vertex detector," *IEEE Trans. Nucl. Sci.*, vol. 37, p. 1120, 1990.
- [4] W. R. Th. Ten Kate, "The influence of the strip width on the performance of a strip detector," *Nucl. Instr. Meth.*, vol. A253, p. 333, 1987.
- [5] M. Kubota, T. Ohsugi, M. Ishizuka *et al.*, "Radiation damage of double-sided silicon strip detectors," *Conference record of the 1991 IEEE Nucl. Sci. Symposium*, Santa Fe, New Mexico, Nov. 2-9, p. 246, 1991.
- [6] K. Saito, M. Nakamura, K. Teraoka *et al.*, "Development and test of a double sided silicon strip detectors," *Conference record of the 1991 IEEE Nucl. Sci. Symposium*, Santa Fe, New Mexico, Nov. 2-9, p. 289, 1991.

- [7] H. Ikeda, M. Tanaka, and S. Okuno, "Detector capacitance of silicon microstrip detector," *Nucl. Instr. Meth. Phys. Res.*, vol. A313, pp. 31–36, 1993, KEK Preprint 91-122. October (1991), to be published *Nucl. Instr. Meth.*
- [8] G. Hall, D. Vité, and R. Wheadon, "Calculation of the geometrical capacitance of silicon microstrip structures using a variational approach," *Nucl. Instr. Meth. Phys. Res.*, vol. A326, pp. 228–233, 1993, Presented at the Sixth Symposium on Semiconductor Detector, Milano, February 1992.
- [9] C. Levier, UC Santa Cruz preprint SCIPP 92/26.
- [10] K. Yamamoto, K. Yamamura, K. Saito, M. Konmura, M. Nakamura, and K. Niwa, "A study on the inter-strip capacitance of double sided silicon strip detector," Presented at the Sixth Symposium on Semiconductor Detector, Milano, Feb. 1992.
- [11] M. Caccia, L. Evensen, T. E. Hansen, R. Horisberger, L. Hubbeling, A. Peisert, T. Tuuva, P. Weilhammer, and A. Zalewska, "A Si strip detector with integrated coupling capacitors," *Nucl. Instr. Meth.*, vol. A243, p. 153, 1986.